No. 136/2025, 7–19
ISSN 2657-6988 (online)
ISSN 2657-5841 (printed)
DOI: 10.26408/136.01

Submitted: 10.10.2025
Accepted: 06.11.2025
Published: 29.12.2025

ANALYSIS OF STRENGTH PROPERTIES OF SELECTED MATERIALS FOR 3D PRINTING

Patryk Krawulski[1*], Sylwia Bazychowska[2], Włodzimierz Kończewicz[3], Bartosz Adamkiewicz[4]

[1,2,3,4] Gdynia Maritime University, Morska 81–87, 81-225 Gdynia, Poland

[1] ORCID 0000-0002-7093-6627, e-mail: p.krawulski@wm.umg.edu.pl

[2] ORCID 0000-0002-9074-9810

[3] ORCID 0000-0001-7180-5533

*Corresponding author

Abstract: 3D printing is now becoming an integral part of technological development worldwide. The growing popularity of additive techniques means that more and more money is being spent on them, and their applications are gradually extending into more areas of life. Incremental manufacturing makes it possible to produce both prototypes and finished spare parts, the properties of which are comparable, and often almost identical, to components currently in use. With this technology, it is possible to create components with complex geometries without having to invest in costly, advanced mass production. 3D printing technologies make it possible to construct three-dimensional objects based on successive layers of material. Testing of the additive-printed samples was carried out using an orthogonal plan, in which factors are selected so that each is different from the others. This means that during the experiments, the influence of the individual parameters could be assessed independently, without interference from other variables. As part of the study, specimens were prepared and subjected to a static tensile test. The test models were printed with five different infill densities: 20; 40; 60; 80; and 100. After testing, the results obtained were collated in the form of graphs illustrating, among other things, the tensile strength of the Young's modulus values and the percentage strain. These data were then analysed and described in detail for all selected materials. The highest tensile strength value was obtained for the PET-G material with 50.09 MPa at 100% infill. The lowest tensile strength value was achieved by the ASA material – 23.43 MPa at 20% infill. The highest Young's Modulus value was achieved by the ASA material – 1924 MPa at 100% infill. The lowest value of the Young's Modulus was obtained for the PET-G material – 934 MPa at 20% infill. The material and the infill density have no significant effect on the deformation value. The results showed that changing the infill density has an effect on the strength properties.

Keywords: 3D printing, material property analysis, FDM, strength properties, additive technologies.

1. INTRODUCTION

Classified as an additive manufacturing process, 3D printing technology has revolutionised the design and manufacture of components, offering an alternative to traditional cavity machining or injection moulding [Zhou et al. 2024]. One of the most popular and widely used additive techniques is FDM (Fused Deposition Modelling), which has found applications both in industry and with hobbyists due to its accessibility, relatively low running costs and wide range of materials [Turner, Strong and Gold 2014]. This method is based on a controlled extrusion process of thermoplastic filament – the material in the form of a thin strip is fed into a heated head (hotend), where it is plasticised and then precisely deposited layer by layer on the work platform [Sood, Ohdar and Mahapatra 2010]. The result is the successive construction of a three-dimensional geometry conforming to a digital CAD model, previously processed by slicer software into a set of G-code instructions [Boschetto and Bottini 2014].

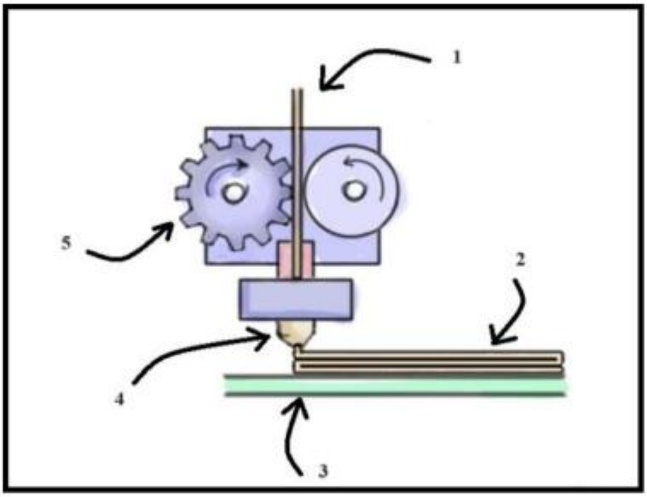

Fig. 1. Layer-by-layer deposition scheme: 1 – thermoplastic filament, 2 – first layers of printed object, 3 – work table, 4 – print head, 5 – extruder drawing the filament to the print head

A key feature of FDM technology (Fig. 1) is the ability to adjust the process parameters – such as the extruder temperature, work table temperature, print speed, layer height and infill density – which directly affect the mechanical properties, dimensional accuracy and aesthetics of the finished prints [Sood, Ohdar and Mahapatra 2010]. This allows users to consciously balance the lead time with the surface quality and durability of the component [Chacón et al. 2017]. Choosing the right material is also crucial. Polymers such as PLA, PETG, ABS and nylon differ in their mechanical properties [Wojtyła, Klama and Baran 2017], chemical and thermal resistance and printing requirements, opening up a wide range of applications – from conceptual prototypes and functional components to structural components operating in harsher environments [Rane and Strano 2019]. The study focuses on comparing samples made from different polymer filaments at varying infill densities to determine their effects on tensile strength, Young's modulus and strain. The results obtained form the basis for optimising material selection and printing parameters for specific functional applications.

2. RESEARCH METHODOLOGY

Filaments were used to produce the samples: ASA and PET-G with a diameter of 1.75 mm, purchased from Fiberlogy. The fabricated specimens (Fig. 2) were made with the given parameters (Tab. 1), which were produced using an Original Prusa XL 5T 3D printer (Fig. 3). The static tensile test specimens were made in accordance with PN-ISO 5893:2015–12 [Kończewicz et al. 2022; Krawulski and Dyl 2023] (Fig. 4). The laboratory static tensile tests were performed on a Zwick & Roell 100 kN testing machine. In the experiment carried out, the influence of the type of material and the infill density on the mechanical properties of the samples was subjected to testing without changing the other process parameters. All specimens were printed in an orientation in line with the longitudinal axis of the specimen (horizontal direction, parallel to the working table), thus reducing the influence of anisotropy due to the direction of layering and ensuring comparability of results.

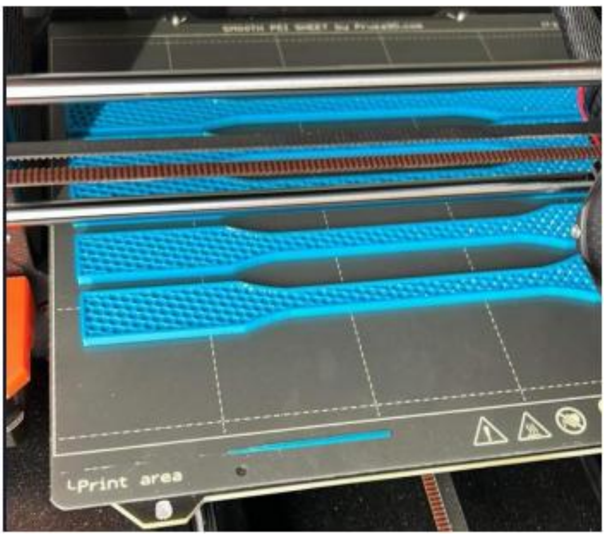

Fig. 2. Samples shown during printing

Table 1. Applied printing parameters

Parameter	ASA	PET-G
Temp. Nozzles [°C]	255–270	220–250
Temp. Table [°C]	90–110	90
Ventilation	Yes	Yes
Infill template	Honeycomb	Honeycomb
Infill density [%]	20/40/60/80/100	20/40/60/80/100
Printing speed [mm/s]	<100	<100
Layer height [mm]	0–15	0–15
Nozzle diameter [mm]	0–4	0–4
Additional adhesive	Yes	Yes

Fig. 3. Original Prusa IMK3S+ 3D printer

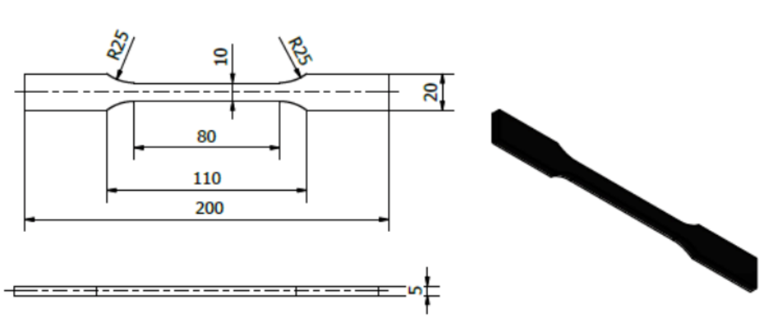

Fig. 4. Dimensions of strength test specimens

3. TEST RESULTS

In order to analyse the selected filaments, graphs are presented for the tensile test, Young's modulus and strain versus infill density of the printed samples.

3.1. ASA material

The graph (Fig. 5) shows the measured results of the tensile strength R_m [MPa] in relation to the infill density of the sample p [%].

Table 2 considers the tensile strength values R_m [MPa] from the infill density of the samples.

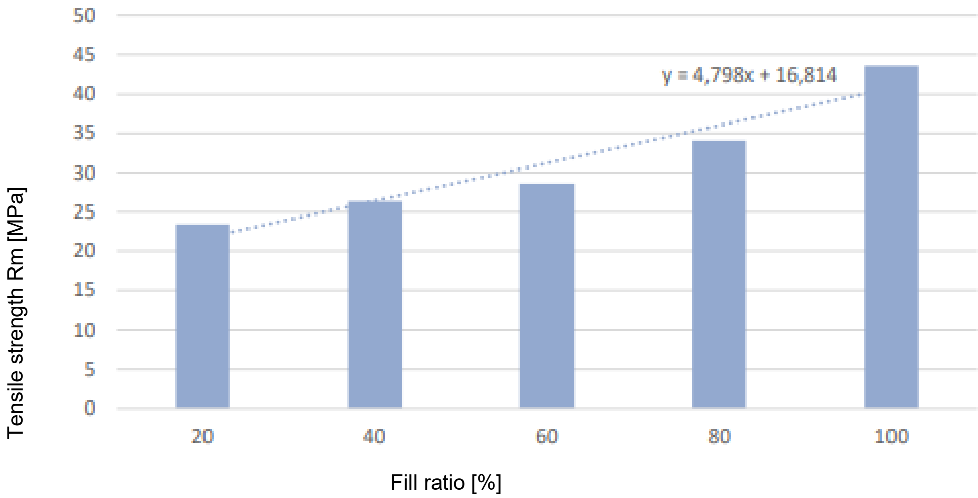

Fig. 5. Diagram of the dependence of the tensile strength on the infill density of the specimens

Table 2. Summary of test results for tensile strength Rm [MPa]

Fill ratio [%] p [%]	20	40	60	80	100
Tensile strength Rm [MPa] R_m [MPa]	23–43	26–37	28–59	34–09	43–56

The highest tensile strength value was achieved by specimens printed with 100% infill. The lowest tensile strength value was achieved by samples with a 20% infill. At 20% infill, the tensile strength is 23.43 MPa, while at maximum infill it is 43.56 MPa. It is concluded that an increase in material strength occurs with an increase in the infill density.

The graph (Fig. 6) shows the results of the Young's Modulus [MPa] versus the infill density of the specimens *p* [%]. The strain values are listed in Table 3.

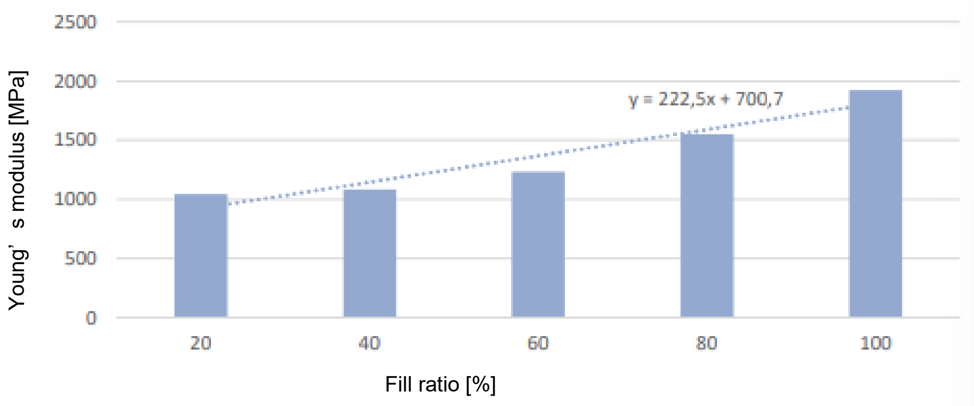

Fig. 6. Graph of the dependence of Young's modulus on the infill density

Table 3. Summary of the Young's Modulus [MPa] results obtained

Fill ratio [%] ***p*** **[%]**	20	40	60	80	100
Young's modulus [MPa]	1046	1084	1234	1553	1924

The graph (Fig. 7) shows the results for the strain [%] versus the specimen printing angle.

The strain values are listed in Table 4.

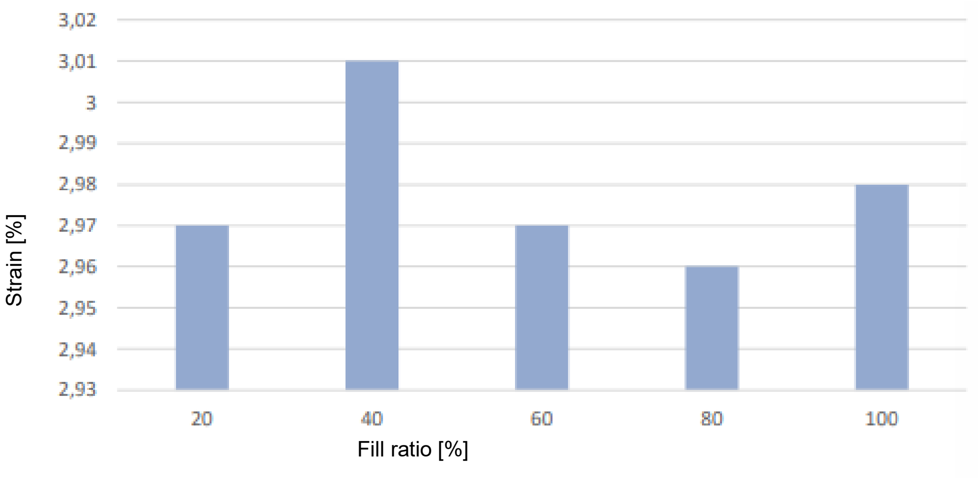

Fig. 7. Diagram of the relationship of strain to change in infill density

Table 4. Summary of test results for strain

Fill ratio [%] p **[%]**	20	40	60	80	100
Strain [%]	2–97	3–01	2–97	2–96	2–98

In the case of the deformation parameter, a relationship was observed which indicates that similar and comparable results are obtained at all infill densities.

3.2. PET-G material

The graph (Fig. 8) shows the measured results of the tensile strength R_m [MPa] in relation to the infill density of the sample p [%].

Table 5 considers the tensile strength values R_m [MPa] from the infill density of the samples.

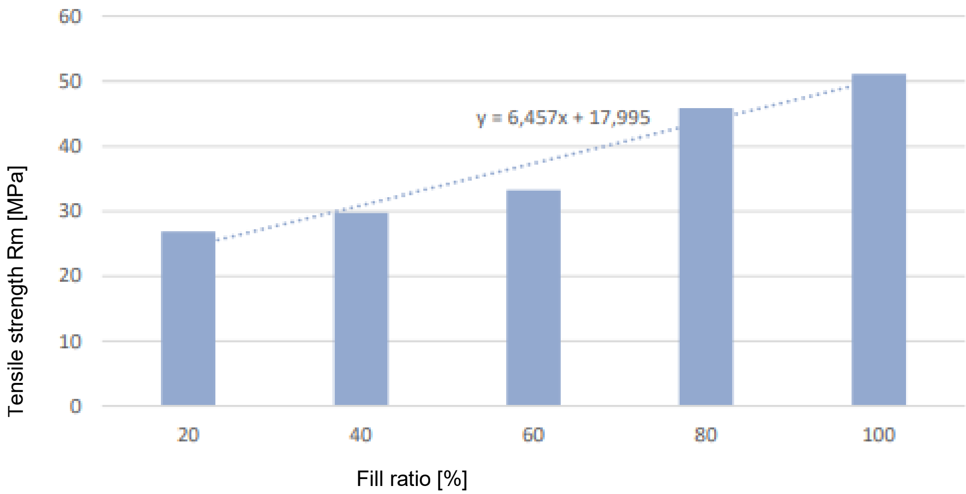

Fig. 8. Diagram of the dependence of the tensile strength on the infill density of the specimens

Table 5. Summary of test results for tensile strength Rm [MPa]

Fill ratio [%] p **[%]**	20	40	60	80	100
Tensile strength Rm [MPa] R_m **[MPa]**	26–85	29–79	33–22	45–88	51–09

The highest tensile strength value was achieved by specimens printed with 100% infill. The lowest tensile strength value was achieved by samples with a 20% infill. At 20% infill, the tensile strength is 26.85 MPa, while at maximum infill it is 51.09 MPa. It is concluded that an increase in material strength occurs with an increase in the infill density.

The graph (Fig. 9) shows the results of the Young's Modulus [MPa] versus the infill density of the specimens p [%].

The strain values are listed in Table 6.

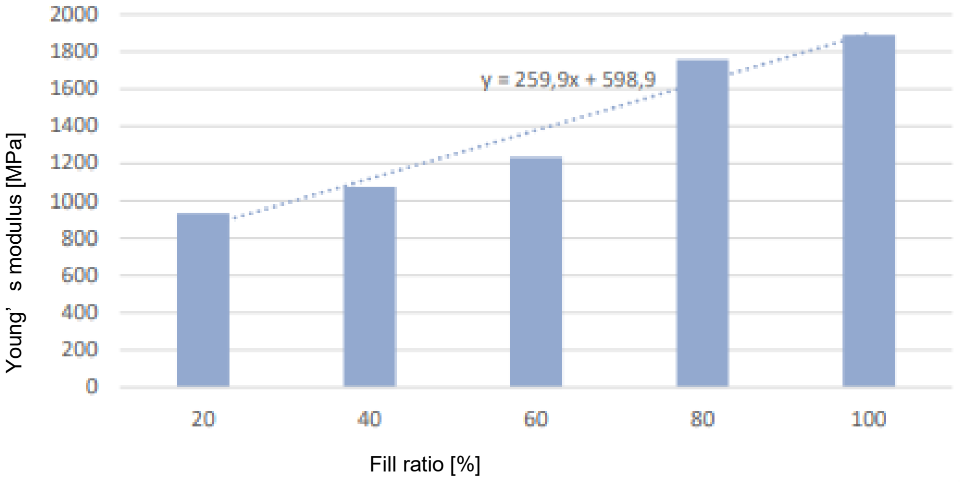

Fig. 9. Graph of the dependence of Young's modulus on the infill density

Table 6. Summary of test results for tensile strength Rm [MPa]

Fill ratio [%] ***p*** **[%]**	20	40	60	80	100
Young's modulus [MPa]	934	1075	1234	1758	1892

The graph (Fig. 10) shows the results for the strain [%] versus the specimen printing angle.

The strain values are listed in Table 7.

Table 7. Summary of test results for strain

Fill ratio [%] ***p*** **[%]**	20	40	60	80	100
Strain [%]	3–90	3–71	3–67	3–66	3–82

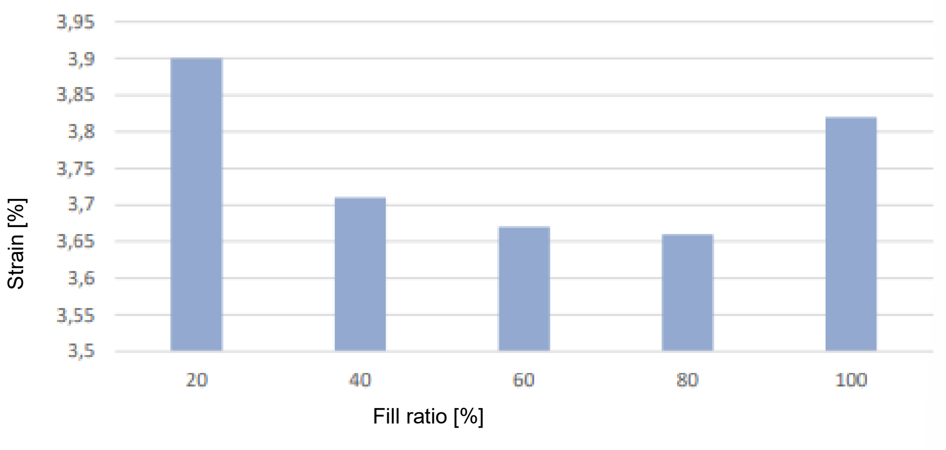

Fig. 10. Diagram of the relationship of strain to change in infill density

Table 8 lists the test results obtained for the specimens as a function of changes in the printing angle and temperature.

Table 8. Summary of the results obtained for the samples depending on the infill density

Infill [%]	Rm [MPa]		Young's modulus [MPa]		Strain [%]	
	ASA	PET-G	ASA	PET-G	ASA	PET-G
20	23–43	26–85	1046	934	2–97	3–90
40	26–37	29–79	1084	1075	3–01	3–71
60	28–59	33–22	1234	1234	2–97	3–67
80	34–09	45–88	1553	1758	2–96	3–66
100	43–56	51–09	1924	1892	2–98	3–82

The graph (Fig. 11) is a comparison of the test results for tensile strength.

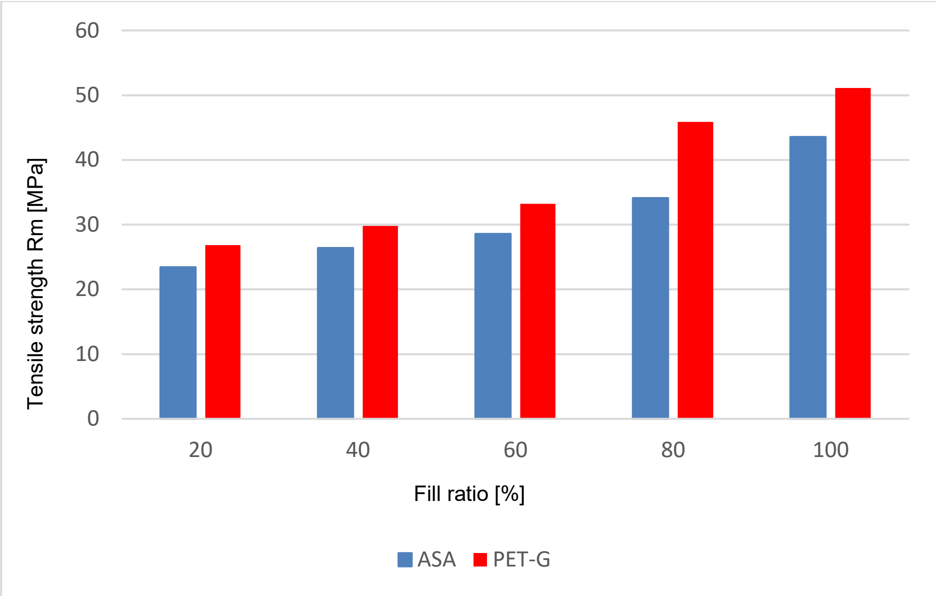

Fig. 11. Tensile strength comparison graph

The graph (Fig. 12) is a comparison of the test results for Young's modulus.

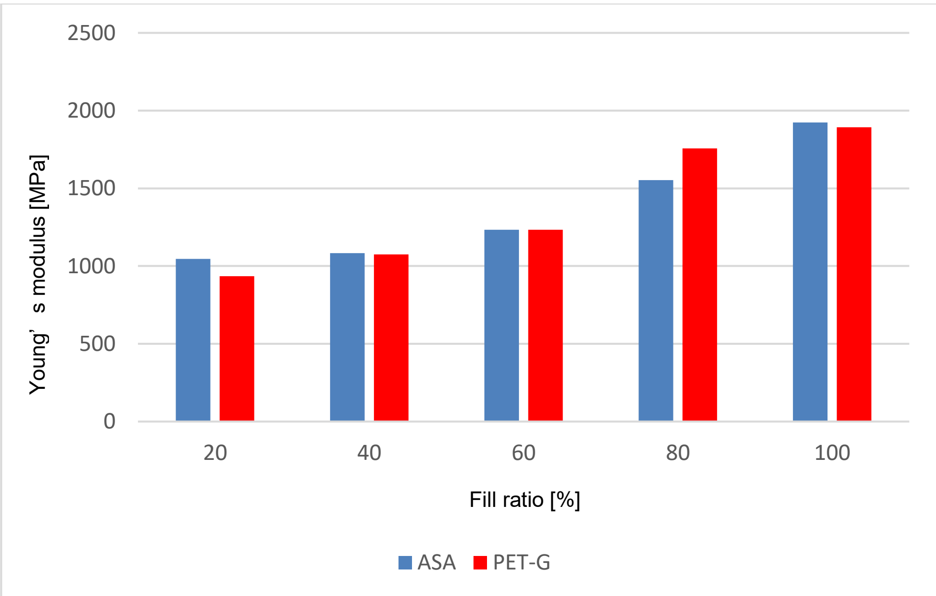

Fig. 12. Comparative graph of Young's modulus [MPa]

The graph (Fig. 13) is a comparison of the test results for Young's modulus.

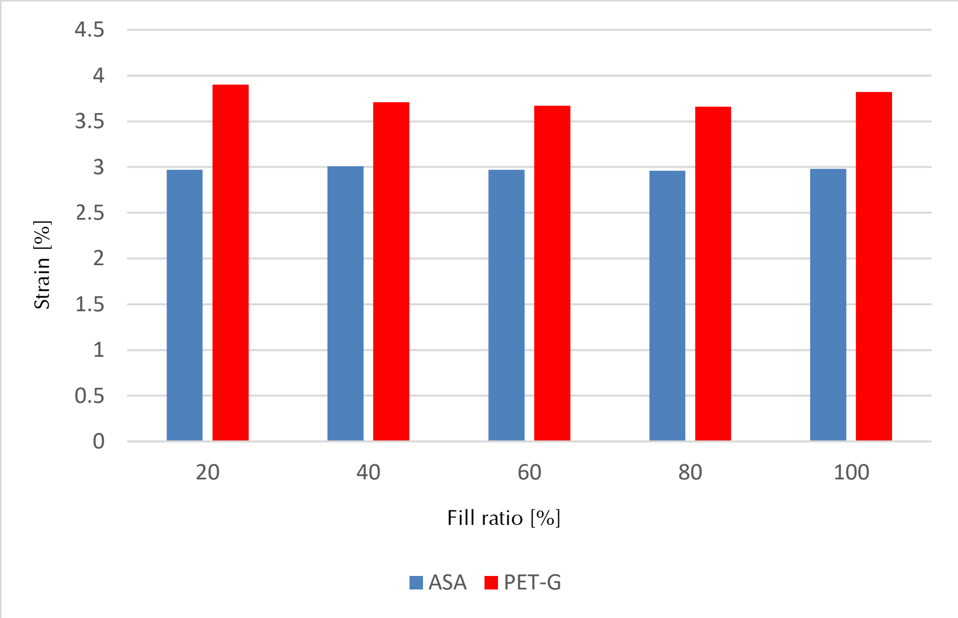

Fig. 13. Comparative graph of deformations [%]

4. CONCLUSIONS

The highest tensile strength value Rm [MPa] was achieved by the PET-G filament at 100% infill – 50.09 MPa. The lowest tensile strength value Rm [MPa] was achieved by the ASA filament at 20% infill – 23.43 MPa.

The highest value of Young's modulus [MPa] was achieved by the ASA filament at 100% infill – 1924 MPa. The lowest value of Young's modulus [MPa] was achieved by the PET-G filament at 20% infill – 934 MPa.

The highest strain value [%] was achieved by the PET-G filament at 20% infill – 3.90%. The lowest strain [%] value was achieved by the ASA filament at 80% infill – 2.96%.

The material and the infill density do not have a significant effect on the deformation, as the result obtained is in the range of 2.96 to 3.90%.

The research carried out showed that the choice of material and the infill density influences the strength properties of the selected filaments.

Analysis of the results has provided a better understanding of the mechanical properties of the selected filaments, which can contribute to further research into optimising the FDM manufacturing process.

REFERENCES

Boschetto, A., Bottini, L., 2014, *Accuracy Prediction in Fused Deposition Modeling*, International Journal of Advanced Manufacturing Technology, vol. 73, pp. 913–928.

Chacón, J.M., Caminero, M.A., García-Plaza, E., Núñez, P.J., 2017, *Additive Manufacturing of PLA Structures Using Fused Deposition Modelling: Effect of Process Parameters on Mechanical Properties and Their Optimal Selection*, Materials & Design, vol. 124, pp. 143–157.

Kończewicz, W., Krawulski, P., Bieszk, A., Darznik, D., 2022, *The Analysis of Properties Selected Filaments for Making Components and Parts of Marine Equipment by Fused Deposition Modelling on Example of Flexible Clutch Coupling and Oli Centrifuge Scroll*, Journal of Konbin, vol. 52, no. 3, pp. 211–221.

Krawulski, P., Dyl, T., 2023, *The Impact of 3D Printing Assumptions and CNC Machining Conditions on the Mechanical Parameters of the Selected PET Material*, Archives of Materials Science and Engineering, vol. 120, pp. 36–41.

Rane, K., Strano, M., 2019, *A Comprehensive Review of FDM: Process Parameters and Materials*, Science and Engineering of Composite Materials, vol. 26, no. 1, pp. 154–172.

Sood, A.K., Ohdar, R.K., Mahapatra, S.S., 2010, *Parametric Appraisal of Mechanical Property of Fused Deposition Modelling Processed Parts*, Materials & Design, vol. 31, no.1, pp. 287–295.

Turner, B.N., Strong, R., Gold, S.A., 2014, *A Review of Melt Extrusion Additive Manufacturing Processes: I. Process Design and Modeling*, Rapid Prototyping Journal, vol. 20, no. 3, pp. 192–204.

Wojtyła, S., Klama, P., Baran, T., 2017, *Is 3D Printing Safe? Analysis of the Thermal Treatment of Thermoplastics: ABS, PLA, PET, and Nylon*, Journal of Occupational and Environmental Hygiene, vol. 14, no. 6, D80–D85.

Zhou, L., Miller, J., Vezza, J., Mayster, M., Raffay, M., Justice, Q., Al Tamimi, Z., Hansotte, G., Sunkara, L.D., Bernat, J., 2024, *Additive Manufacturing: A Comprehensive Review*, Sensors, no. 24.